Characterization of Bacterial Polysaccharide Capsules and Detection in the Presence of Deliquescent Water by Atomic Force Microscopy

Hai-Nan Su, Zhi-Hua Chen, Sheng-Bo Liu, Li-Ping Qiao, Xiu-Lan Chen, Hai-Lun He, Xian Zhao, Bai-Cheng Zhou, and Yu-Zhong Zhang

State Key Laboratory of Crystal Materials and State Key Laboratory of Microbial Technology, Shandong University, Jinan, People's Republic of China

We detected polysaccharide capsules from *Zunongwangia profunda* SM-A87 with atomic force microscopy (AFM). The molecular organization of the capsules at the single-polysaccharide-chain level was reported. Furthermore, we found that with ScanAsyst mode the polysaccharide capsules could be detected even in the presence of deliquescent water covering the capsule.

Capsular polysaccharide (CPS) plays important biological roles for many microorganisms, such as nutrient uptake (17), protection against environmental stresses (15), biofilm formation (8), and survival against phagocytosis or antibiotics (3, 19, 20). Moreover, CPS is potentially economically important material (2, 6, 7). Thus, detection and analysis of bacterial capsules are required for understanding of the physiology, ecology, and toxicity of the relative bacteria.

Atomic force microscopy (AFM) has been used in microbiological research for nearly 20 years (21), and this method is widely used in detecting the ultrastructures of microorganisms and associated extracellular materials (for review, see references 5, 14, and 18). Previous work with AFM has revealed liquid-like substances surrounding the bacterial cells under ambient conditions, and these substances used to be considered bacterial capsules (22, 23). However, recent advances have pointed out that these liquid-like structures are in fact deliquescent water instead of real bacterial capsules (13). Thus, identification of the real bacterial capsule under AFM remains elusive.

In this report, we selected the CPS-producing bacterium *Zunongwangia profunda* SM-A87 (formerly named *Wangia profunda* SM-A87) (16) for the capsule research. The strain was cultured as previously described (11). Briefly, the strain was first cultured on a marine agar medium (10 g/liter peptone, 5 g/liter yeast extract, 15 g/liter agar, and artificial seawater) at 30°C for 1 day. Then, the strain was inoculated into an Erlenmeyer flask (250 ml) containing 50 ml basal medium (10 g/liter peptone, 5 g/liter yeast extract, and artificial seawater) and incubated at 30°C at 200 rpm for 1 day. Our previous work indicated that *Z. profunda* SM-A87 could produce more CPS when lactose was used as the carbon source (11); thus, a 5% (vol/vol) inoculum was then added to a flask (500 ml) containing 100 ml basal medium and 3% lactose, and the flask was incubated at 10°C at 200 rpm for 1 week. The final optical density at 600 nm (OD_{600}) usually reached 25 to 55. The bacterial capsules were first examined with the traditional negative-staining method, and the presence of capsules was confirmed before subsequent experiments were conducted (see Fig. S1 in the supplemental material).

To avoid the influence of the introduction of deliquescent water in AFM imaging experiments, the culture of *Z. profunda* SM-A87 bacterial cells was diluted with distilled water instead of biological buffer to at least 10^6-fold. A drop of the bacterial suspension was placed on freshly cleaved mica and kept under ambient conditions for drying. The use of distilled water to prepare the samples would bring about hypoosmotic shock to the

bacteria; for example, there would be a minor increase in cell volume during the dilution process (4). Thus, there would be changes in bacterial morphology. However, extracellular macromolecules such as polysaccharides were less affected by the osmotic shock. AFM images were obtained by using a Multimode Nanoscope VIII AFM (Bruker AXS, Germany) with a J-type scanner. Probe (NSC11; MikroMasch) with a cantilever length of 90 μm and a nominal spring constant of 48 N/m was used. As polysaccharides are usually adhesive, sometimes the tip of the probe was coated with polysaccharide molecules during the imaging process, resulting in reduction of resolution or multiplication of small structures (1). This effect could be eliminated by replacing the probe.

AFM images of the capsulated bacterial cells were then recorded. A typical polysaccharide capsule had a diameter of about 9 μm (Fig. 1A and B). The polysaccharide fibrils at the center of the capsule entangled with each other to form a dense structure. Polysaccharide fibrils in the peripheral area formed a network with a lower degree of cross-linking than in the center area. The polysaccharide capsule was composed of fibrils with different heights. The heights of the thin fibrils were around 0.3 nm (see Fig. S2 in the supplemental material), which were close to the height of a single polysaccharide chain (12). The heights of the thicker fibrils ranged from 0.6 to 0.9 nm (Fig. S2), indicating the association of multipolysaccharide chains.

More than 400 images of capsulated bacterial cells were recorded in our experiments. Most of the capsules that we detected were composed of fibril structures, with diameters ranging from 4 μm to 10 μm. Different amounts of the polysaccharide fibrils around the cells might indicate different stages of polysaccharide secretion (see Fig. S3 in the supplemental material). During our observation, the longest single fibril reached as long as 12 μm, which was 7 to 8 times the length of the bacterial cell (Fig. S4). Apart from polysaccharide fibrils, in some images sheet structures surrounding the bacterial cells were noticed (about 19% of all
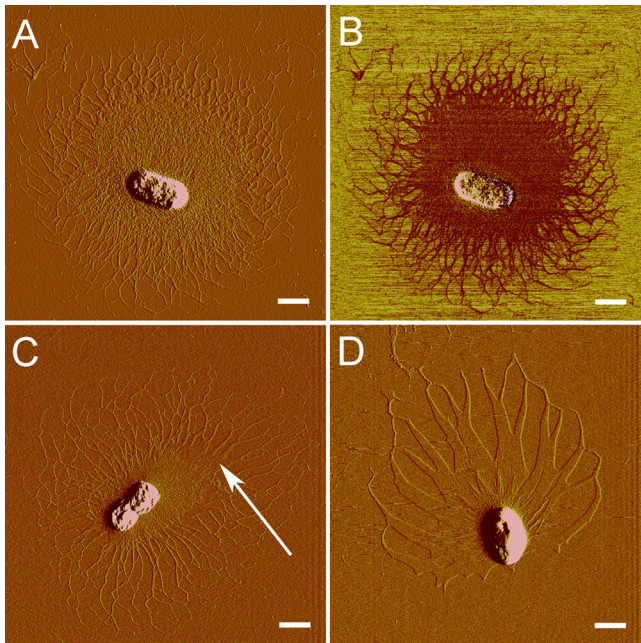
FIG 1 AFM images of *Z. profunda* SM-A87 cells with polysaccharide capsules. The amplitude image (A) and the phase image (B) of a commonly observed capsulated bacterial cell are shown. (C) Amplitude image of a capsulated cell showing that the sheet structures (white arrow) and fibrils coexist in the same capsule. (D) Amplitude image of a capsule that was completely composed of sheet structure. Scale bar, 1 μm.

FIG 2 (A) Two capsulated *Z. profunda* SM-A87 cells imaged with AFM on mica. Polysaccharide fibrils of the capsules were clearly visible. (B) The same *Z. profunda* SM-A87 cells imaged after being rinsed with HEPES buffer and air dried. Polysaccharide capsules of the two bacterial cells were embedded in deliquescent water. Scale bar, 1 μm.

images). In most of these images, fibril structure and sheet structure coexist in the same capsule (Fig. 1C). Only some capsules are completely composed of sheet structure (Fig. 1D). The sheet structures from different images shared similar heights, about 1 nm, and may have originated from the association of polysaccharide fibrils side by side.

Some frequently used biological buffers often contain deliquescent components, such as K_2HPO_4, HEPES, $CaCl_2$, and NaCl (13). The use of these buffers to prepare the samples often brought about the liquids surrounding the bacterial cells. Thus, the influence of deliquescent water on the detection of capsules was tested. First, an area with two typical capsulated bacterial cells on a mica surface was imaged, and the polysaccharide fibrils of the capsules were clearly visible (Fig. 2A). Then, the mica was rinsed with 0.5 mM HEPES buffer. After the mica was air dried, the same two bacterial cells were imaged again. As shown in Fig. 2B, the capsules were completely covered by deliquescent water. Thus, it was shown that deliquescent components in the biological buffers seriously influenced the detection of bacterial capsules with AFM.

Thus, in the presence of deliquescent water, how to detect polysaccharide capsules remains an unresolved problem. To eliminate the influence of deliquescent water on the detection of bacterial capsules with AFM, different AFM scanning modes were tested to image the same capsulated bacterial cell, which was suspended by 0.5 mM HEPES buffer and then fully air dried. The bacterial sample was first imaged in the most commonly used tapping mode (Fig. 3A to D). It was noticed from the results that the bacterial cell was covered by deliquescent water, and no capsular polysaccharide fibril structures were visualized. Then, we imaged the same bacteria with a newly available scanning mode,
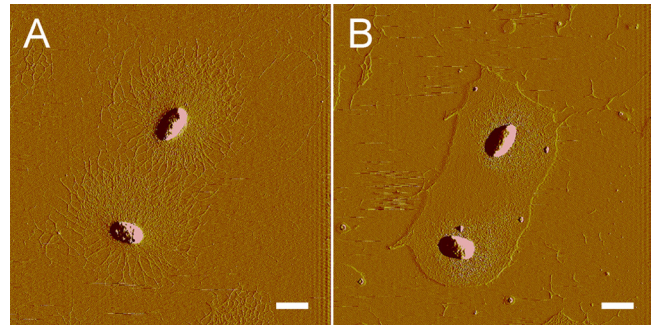
ScanAsyst mode. The operation of AFM in ScanAsyst mode followed the standard imaging method described by the manufacturer (10). In contrast to what was observed for tapping mode, in which the same cell was imaged again, not only was the deliquescent water covering the bacterial cell detected, but the capsule covered by deliquescent water was also successfully detected (Fig. 3E to G). In the peripheral area of the capsule, even a single polysaccharide fibril was clearly visualized (see Fig. S5 in the supplemental material). The polysaccharide fibrils of the capsule embedded in deliquescent water were traced both in height and in peak force error image. Therefore, it was found that the bacterial capsules could be detected when covered by deliquescent water in ScanAsyst mode.

Section analysis was carried out to compare the results obtained from tapping mode and ScanAsyst mode. The height of the bacteria was about 250 nm, and the diameter of the bacterial capsule was about 5 μm (Fig. 4A). The results obtained from different scanning modes were similar. However, the measured heights of the capsules were different between different scanning modes. For example, the highest point in the section analysis results for the position indicated in Fig. 3 for ScanAsyst mode was 13.5 nm (Fig. 4B), which was less than 80% of the value obtained with tapping mode (Fig. 4B), showing a great reduction of measured height.

ScanAsyst mode is a newly available commercial technology. It is based on peak force tapping mode (Bruker AXS), which performs a force curve at every single pixel in the image when imaging the sample, and the peak force of the curve was used as the imaging feedback signal (9, 10). Critical imaging parameters could then be automatically adjusted by the instrument when operated in ScanAsyst mode, and the applied force could be minimized at all points of the sample on both soft and hard areas (9, 10). Thus, the resolution of the image obtained from ScanAsyst mode was usually higher. In this work, the probe tip might have slightly penetrated the surface of the deliquescent water when performing every force curve. When the tip penetrated the water layer, the tip could contact the polysaccharide capsules. Then, the capsules embedded under deliquescent water could be imaged. This could also explain why the measured height of the capsule was lower with ScanAsyst mode than with tapping mode. However, elucidation of the exact mechanism by which polysaccharide fibrils embedded in water could be detected in ScanAsyst mode but not in tapping mode still requires further work. Our experiments show a possible way to
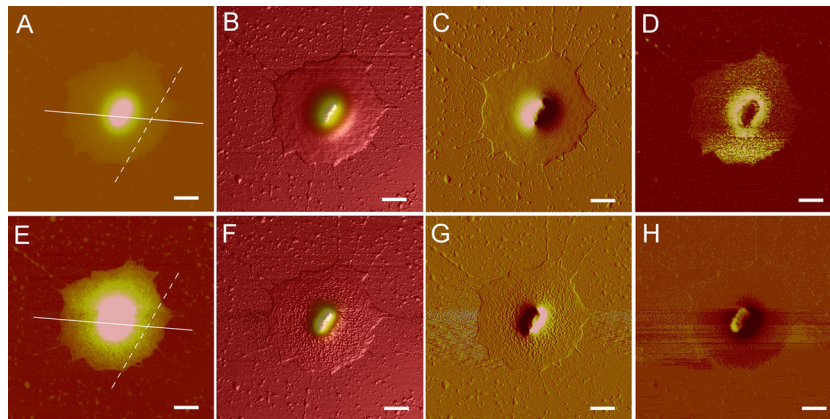
FIG 3 AFM images of a capsulated *Z. profunda* SM-A87 cell embedded in deliquescent water. The height image (A), 3-dimensional height image (B), amplitude image (C), and phase image (D) collected in tapping mode are shown. The height image (E), 3-dimensional height image (F), peak force error image (G), and inphase image (H) collected in ScanAsyst mode are also shown. Lines and dashed lines in panels A and E indicate the positions for cross section analysis shown in Fig. 4. Scale bar, 1 μm.

detect the water film-covered small structures that can hardly be detected by the traditional tapping method with AFM.

For many biological samples, observation in buffer or water will provide researchers with information close to that observed under physiological conditions. Here in our experiments, we successfully detected the capsular fibrils embedded in deliquescent water. It is reasonable to consider that the structure of the capsule detected in this experiment is very close to the natural state of the capsule under physiological conditions.
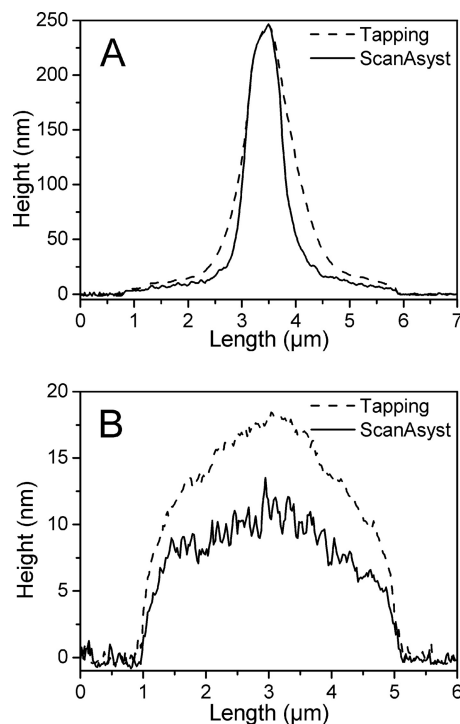
FIG 4 Section analysis of the capsulated bacterial cell covered by deliquescent water as shown in Fig. 3. This analysis was carried out to compare the results obtained from tapping mode and ScanAsyst mode. Panel A shows the cross section indicated with lines in Fig. 3, and panel B shows the cross section indicated with dashed lines in Fig. 3.

Conclusions. Previous work in detecting bacterial capsules usually considered the liquid-like structure around the bacterial cell to be capsule. However, recent progresses have pointed out that the liquid-like structure is actually deliquescent water. Thus, the morphology of bacterial capsules under AFM is still unclear. In this work, the polysaccharide capsule of *Z. profunda* SM-A87 was studied with AFM. The encapsulated bacterial sample was prepared by diluting it with distilled water instead of buffers to avoid introduction of deliquescent water. Subsequently, the morphology and the molecular organization of the capsules at the single-polysaccharide-chain level were successfully recorded with AFM. The typical capsule was found to be formed by polysaccharide fibrils at different association degrees. The commonly seen sheet structure was also characterized. Furthermore, it was found that deliquescent components such as HEPES indeed brought about deliquescent water, which would cover the capsules and influence detection of the capsules. However, we found that with a newly available technique, ScanAsyst mode, the polysaccharide capsules could be detected even in the presence of deliquescent water covering the capsule. The capsular polysaccharide fibrils embedded in water provided us with the information of capsular structures at near physiological conditions, showing the natural molecule organization of the capsules.

REFERENCES

1. **Abu-Lail NI, Camesano TA.** 2003. Polysaccharide properties probed with atomic force microscopy. J. Microsc. **212**:217–238.
2. **Becker A, Katzen F, Puhler A, Ielpi L.** 1998. Xanthan gum biosynthesis and application: a biochemical/genetic perspective. Appl. Microbiol. Biotechnol. **50**:145–152.
3. **Campos MA, et al.** 2004. Capsule polysaccharide mediates bacterial resistance to antimicrobial peptides. Infect. Immun. **72**:7107–7114.
4. **Csonka LN.** 1989. Physiological and genetic responses of bacteria to osmotic stress. Microbiol. Rev. **53**:121–147.

5. **Dufrêne YF.** 2008. Towards nanomicrobiology using atomic force microscopy. Nat. Rev. Microbiol. **6**:674–680.

6. **Fialho AM, et al.** 2008. Occurrence, production, and applications of gellan: current state and perspectives. Appl. Microbiol. Biotechnol. **79**:889–900.

7. **Gutnick DL.** 1987. The emulsan polymer: perspectives on a microbial capsule as an industrial product. Biopolymers **26**:S223–S240.

8. **Houdt RV, Michiels CW.** 2005. Role of bacterial cell surface structures in *Escherichia coli* biofilm formation. Res. Microbiol. **156**:626–633.

9. **Kaemmer SB.** 2011. Introduction to Bruker's ScanAsyst and PeakForce tapping AFM technology. Bruker application note. Bruker Nano Inc., Santa Barbara, CA.

10. **Kelley V.** 2010. Vecco Multimode VIII instruction manual. Bruker Nano Inc., Santa Barbara, CA.

11. **Liu S-B, et al.** 2011. Optimization of fermentation conditions and rheological properties of exopolysaccharide produced by deep-sea bacterium *Zunongwangia profunda* SM-A87. PLoS One **6**:e26825.

12. **McIntire TM, Brant DA.** 1999. Imaging of carrageenan macrocycles and amylose using noncontact atomic force microscopy. Int. J. Biol. Macromol. **26**:303–310.

13. **Méndez-Vilas A, Labajos-Broncano L, Perera-Núñez J, González-Martín ML.** 2011. Are the soft, liquid-like structures detected around bacteria by ambient dynamic atomic force microscopy capsules? Appl. Environ. Microbiol. **77**:3102–3114.

14. **Müller DJ, Dufrêne YF.** 2008. Atomic force microscopy as a multifunctional molecular toolbox in nanobiotechnology. Nat. Nanotechnol. **3**:261–269.

15. **Ophir T, Gutnick DL.** 1994. A role for exopolysaccharides in the protection of microorganisms from desiccation. Appl. Environ. Microbiol. **60**:740–745.

16. **Qin Q-L, et al.** 2007. *Wangia profunda* gen. nov., sp. nov., a novel marine bacterium of the family *Flavobacteriaceae* isolated from southern Okinawa Trough deep-sea sediment. FEMS Microbiol. Lett. **271**:53–58.

17. **Roberts IS.** 1996. The biochemistry and genetics of capsular polysaccharide production in bacteria. Annu. Rev. Microbiol. **50**:285–315.

18. **Scheuring S, Dufrêne YF.** 2010. Atomic force microscopy: probing the spatial organization, interactions and elasticity of microbial cell envelopes at molecular resolution. Mol. Microbiol. **75**:1327–1336.

19. **Shelburne CE, et al.** 2007. The spectrum of antimicrobial activity of the bacteriocin subtilosin A. J. Antimicrob. Chemother. **59**:297–300.

20. **Smith HE, et al.** 1999. Identification and characterization of the *cps* locus of *Streptococcus suis* serotype 2: the capsule protects against phagocytosis and is an important virulence factor. Infect. Immun. **67**:1750–1756.

21. **Southam G, et al.** 1993. Transmission electron microscopy, scanning tunneling microscopy, and atomic force microscopy of the cell envelope layers of the archaeobacterium *Methanospirillum hungatei* GP1. J. Bacteriol. **175**:1946–1955.

22. **Stukalov O, Korenevsky A, Beveridge TJ, Dutcher JR.** 2008. Use of atomic force microscopy and transmission electron microscopy for correlative studies of bacterial capsules. Appl. Environ. Microbiol. **74**:5457–5465.

23. **Suo Z, et al.** 2007. HEPES-stabilized encapsulation of *Salmonella typhimurium.* Langmuir **23**:1365–1374.